International Journal of Heat and Fluid Flow 29 (2008) 1309–1318

Contents lists available at ScienceDirect

International Journal of Heat and Fluid Flow

journal homepage: www.elsevier.com/locate/ijhff

Numerical investigation of convective heat transfer in unsteady flow past two cylinders in tandem arrangements

Necati Mahir, Zekeriya Altaç *

Eskişehir Osmangazi University, School of Engineering and Architecture, Mechanical Engineering Department, 26480 Batı Meşelik, Eskişehir, Turkey

ARTICLE INFO

Article history:
Received 10 August 2007
Received in revised form 19 December 2007
Accepted 6 May 2008
Available online 20 June 2008

Keywords:
Heat transfer
Numerical simulation
Tandem arrangement
Flow past cylinder
Fluent

ABSTRACT

Unsteady laminar convective heat transfer from two isothermal cylinders of tandem arrangement is numerically investigated. The numerical simulations were carried out by the commercial CFD software—FLUENT®. The working fluid is air. The analysis is carried out for the Reynolds numbers of 100 and 200 and for center-to-center distance ratio, L/D, of 2, 3, 4, 5, 7 and 10. The flow parameters such as the lift and drag coefficients and Strouhal number are also obtained and compared with those of available in the literature. The vorticity and isotherms were generated to interpret the flow and heat transport visualization. The mean and local Nusselt numbers for the upstream and downstream cylinders were obtained. It is found that the mean Nusselt number of the upstream cylinder approaches to that of an single isothermal cylinder for $L/D > 4$ and the mean Nusselt number of the downstream cylinder is about 80% of the upstream cylinder.

1. Introduction

Forced convection heat transfer around circular cylinders has numerous applications in engineering practice such as heat exchangers, space heating, flow around arrays of nuclear fuel rods, heat losses from high-rise buildings, chimneys, power generators, and other thermal applications.

The studies involving flow over two cylinders have been the subject of numerous experimental and numerical work in the last two decades. Both the flow field and force coefficients depend highly on the configuration and the spacing of the cylinder pair due to both wake and proximity-induced interference effects. Some of the earliest experimental studies on cylinder pairs in a tandem orientation that were carried out by Kostic and Oka (1972), Tanida et al. (1973) and King and Johns (1976) demonstrated the presence of two major flow regimes with a complex transition region between them. For closely spaced cylinders, the flow separates behind the first cylinder and reattaches to the second one while, for larger spacing, vortex shedding occurs behind both cylinders.

Extensive reviews of results in tandem, side-by-side and/or staggered arrangements can be found in the published works of Zdravkovich (1977, 1985), Chen (1987), Blevins (1990) and Sumner et al. (2000). Critical spacing, which is defined as the minimum gap between the walls of the cylinders, separating different flow regimes was established for tandem arrangements as well. In tandem arrangement, the numerical studies also confirm the experimental findings; that is, if the gap is greater than the critical spacing ($\sim 3.5D - 3.8D$), the upstream cylinder sheds vortices onto the downstream cylinder. Alternatively, vortex shedding does not occur from the upstream cylinder if the gap is less than the critical spacing.

Mittal et al. (1997) numerically studied incompressible flows past a pair of cylinders at Reynolds numbers 100 and 1000 in tandem and staggered arrangements using a stabilized finite element formulation. In tandem configuration, the center-to-center distance ratio (L/D) was kept at 2.5 and 5.5. The Strouhal number, based on the dominant frequency in the time history of the lift coefficient, for both cylinders was the same. Farrant et al. (2001) studied two-dimensional unsteady incompressible flows around circular cylinders at Reynolds number 100 and 200. A hybrid boundary element method was used to discretize the spatial domain together with a second order implicit finite difference approximation in time. Meneghini et al. (2001) also numerically studied the two-dimensional shedding of vortices and flow interference between two circular cylinders in tandem and side-by-side arrangements. The simulations were performed for Reynolds numbers from 100 to 200. Kondo and Matsukuma (2005) numerically studied two- and three-dimensional flow around two circular cylinders in tandem arrangement for $Re = 1000$. The center-to-center distance between the two cylinders was $2D$ to $5D$. They observed the critical distance to be between $3.5D$ to $4D$. The numerical results were qualitatively compared with experimental data. Carmo and Meneghini (2006) investigated two- and three-dimensional simulations of the incompressible flow around a pair of circular cylinders in tandem arrangements using the spectral element

* Corresponding author. Tel.: +90 222 2393750x3365; fax: +90 222 2393613.
E-mail addresses: nmahir@ogu.edu.tr (N. Mahir), zaltac@ogu.edu.tr (Z. Altaç).

0142-727X/$ - see front matter © 2008 Elsevier Inc. All rights reserved.
doi:10.1016/j.ijheatfluidflow.2008.05.001

method. The centre-to-centre distance of the investigated configurations was varied from 1.5D to 8D. The simulations were in the Reynolds number range from 160 to 320. Ding et al. (2007) numerically studied the flow field around two circular cylinders arranged in side-by-side and tandem configuration (L/D = 2.5 and 5.5) using the mesh-free least square-based finite difference method. The flow simulations were carried out for Re = 100 and 200.

As to the heat transfer from the cylinders, Jue et al. (2001) investigated the convection heat transfer of flow across three heated cylinders arranged in an isosceles right-angled triangle between two parallel plates. The variations of the drag coefficient and time-averaged Nusselt number around the surface of the three cylinders were investigated. In their study, L/D ratio of 0.5–1.25, Reynolds number of 100–300 and Grashoff number of 80,000–200,000 were considered. Buyruk (2002) numerically studied the heat transfer from two isothermal tandem cylinders in cross flow of air at Re = 400. In the study, three staggered isothermal cylinder and four inline isothermal cylinder configurations were also investigated for Re = 80, 120 and 200. Rahnama and Hadi-Moghaddam (2005) numerically investigated 2D unsteady laminar flow past a heated square cylinder mounted inside a plane channel. The blockage ratio was chosen as 1/8 and the Reynolds number was less than 200. The time-averaged Nusselt number, drag coefficient, recirculation length, and Strouhal number were obtained and compared with the literature. Zhou and Yiu (2006) experimentally investigated the flow structure, momentum and heat transport in the wake of two tandem circular cylinders involving the heated upstream cylinder. Their measurements were, however, conducted for Re = 7000 and for L/D = 1.3, 2.5, 4, 6, 10, 20 and 30. They showed that the cross-stream distributions of the Reynolds stresses and heat fluxes at a given x/D vary from one to another. The momentum and heat transport characteristics were then summarized for each flow structure.

It is known that vortex shedding occurs in the wake of a circular cylinder if the Reynolds number is sufficiently large. The vortex shedding affects the heat transfer characteristics of a cylinder. However, the combined wake behind multiple cylinders is different from that of a single circular cylinder; thereby, the influence of the flow interaction between multiple cylinders on heat transfer needs to be further investigated. Thus, the purpose of this study is to numerically investigate the convection heat transfer characteristics of two cylinders of equal diameter in tandem arrangements subject to cross flow of air. The local Nusselt numbers and mean Nusselt numbers for the upstream and downstream cylinders are computed and analyzed with respect to the flow patterns.

2. Governing equations

The governing equations, for unsteady incompressible viscous flow, are

for continuity

$$\frac{\partial u}{\partial x}+\frac{\partial v}{\partial y}=0, \tag{1}$$

for the momentum

$$\frac{\partial u}{\partial t}+u\frac{\partial u}{\partial x}+v\frac{\partial u}{\partial y}=-\frac{1}{\rho}\frac{\partial p}{\partial x}+\nu\left(\frac{\partial^2 u}{\partial x^2}+\frac{\partial^2 u}{\partial y^2}\right), \tag{2}$$

$$\frac{\partial v}{\partial t}+u\frac{\partial v}{\partial x}+v\frac{\partial v}{\partial y}=-\frac{1}{\rho}\frac{\partial p}{\partial y}+\nu\left(\frac{\partial^2 v}{\partial x^2}+\frac{\partial^2 v}{\partial y^2}\right), \tag{3}$$

and for the energy

$$\frac{\partial T}{\partial t}+u\frac{\partial T}{\partial x}+v\frac{\partial T}{\partial y}=\alpha\left(\frac{\partial^2 T}{\partial x^2}+\frac{\partial^2 T}{\partial y^2}\right), \tag{4}$$

where u and v are the velocity components, p is the pressure, ν is the kinematic viscosity, ρ is the density, T is the temperature of the fluid, and α is the thermal diffusivity defined as $k/\rho c$ where k is the thermal conductivity and c is the specific heat of the fluid.

The computational domain and the configuration of the cylinders are illustrated in Fig. 1. The boundary conditions can be stated as:

For the inlet, $u = U_\infty$, $T = T_\infty$,

For the outlet, $\frac{\partial u}{\partial x}=0$, $\frac{\partial v}{\partial x}=0$, $\frac{\partial T}{\partial x}=0$,

For the top and bottom, $u = U_\infty$, $v = 0$, $T = T_\infty$,

For the cylinders walls, $u = 0$, $v = 0$, $T = T_w$,

where U_∞ and T_∞ are the free-stream velocity and temperature and T_w is the cylinder wall temperature which is constant.

The lift and drag coefficients are computed from

$$C_L=\frac{2F_y}{\rho D U_\infty^2}, \qquad C_D=\frac{2F_x}{\rho D U_\infty^2}, \tag{5}$$

where D is the cylinder diameter, F_x and F_y are the force components resolved in the directions x and y.

The Reynolds number is defined as $Re = U_\infty D/\nu$. On the other hand, the local heat transfer coefficient and the local Nusselt number are computed from

$$-k\left.\frac{\partial T}{\partial n}\right|_w=h_\theta(T_w-T_\infty), \qquad Nu_\theta=\frac{h_\theta D}{k}, \tag{6}$$

where n is the direction normal to the cylinder surface; h_θ and Nu_θ are the local heat transfer coefficient and local Nusselt number, respectively; and θ is the polar angle measured in usual counterclockwise direction with respect to cylinder center.

The surface-averaged (mean) Nusselt number is then evaluated as follows:

$$Nu=\frac{1}{2\pi}\int_{\theta=0}^{2\pi} Nu_\theta \,\mathrm{d}\theta, \tag{7}$$

3. Numerical verification

The governing flow and energy equations subjected to the aforementioned boundary conditions are solved using a commercial CFD package—FLUENT®. FLUENT® is capable of handling unsteady Navies-Stokes and energy equations using a finite volume method in two-and three-dimensional geometries (Fluent, 2003).

The first case for the verification of FLUENT simulations is the heat transfer problem of a single isothermal cylinder subject to cross flow of air (Pr = 0.7). The number of grid points and their distribution is an important matter in such unsteady laminar flow over cylinders because of the complex phenomena existing in this type of flow, such as separation and vortex shedding. The compu-

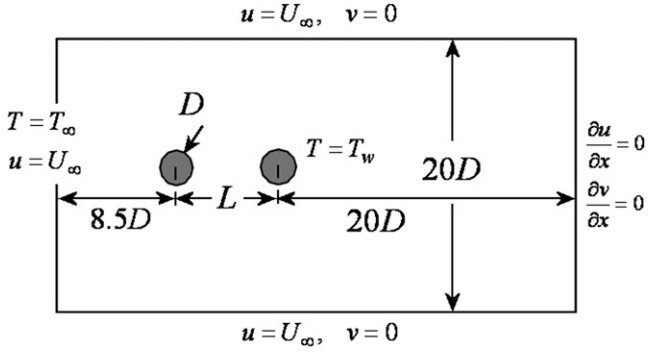

Fig. 1. Computational domain and two cylinder configuration.

tational domain, $20D \times 28.5D$, is meshed using triangular elements. A non-uniform grid distribution was employed with a more refined grid generated around the cylinder wall. The growth rate for the size of the triangular elements was 15% which stretched out to the boundaries of the computational domain (Fig. 2a). The grid was further refined along a rectangular region encompassing the cylinder(s) to accurately capture the wake and vortex street behind the cylinder(s). For this benchmark problem, the total number of elements and nodes were 51 694 and 26 289, respectively. SIMPLE algorithm (Patankar, 1980) along with the second order implicit for time-stepping and three-point second order upwind scheme for the discretization of the convection-diffusion terms was used (Fletcher, 1991). QUICK and Power Law discretizations were not adapted due to the larger computation time and convergence related problems whereas the second order scheme is more robust to tackle fluid flow and heat transfer problems in general. The convergence criterion for the inner (time step) iterations was 10^{-6} for the continuity, momentum and energy equations. The time step was varied from 0.01 to 0.1 to determine an optimum value which resulted in less computational time, yet sufficiently accurate solutions. For $Re = 200$, the Strouhal number (St), drag (C_D) and lift coefficients (C_L), and the mean Nusselt number were obtained and summarized in Table 1. The vortex shedding frequency f is obtained from the Fast Fourier Transform (FFT) of the time-history of the lift coefficient data in order to compute the Strouhal number, fD/U_∞, which is a measure of oscillating fluid. The optimum value for the time step (Δt) was determined to be 0.05 which was adapted in this study.

The Strouhal number, drag and lift coefficients were computed and comparatively tabulated with available numerical and experimental data for $Re = 100$ (in Table 2) and $Re = 200$ (in Table 3). For $Re = 100$ and 200, the Strouhal numbers compare very well with the experimental data of Roshko (1954), Tritton (1959), Norberg (2003) and Williamson (1991). Strouhal numbers for both flow conditions are within the range of the experimental data. The lift and drag coefficients are consistent with those of numerical simulations done by Meneghini (1993), Braza et al. (1986), Ding et al. (2007) and Liu et al. (1998) and the experimental ranges of the lift coefficients Norberg (2003). Besides some shortfalls of the employed numerical schemes, grid structure, etc., we attribute this diversity in the experimental and numerical values to the three-dimensional effects.

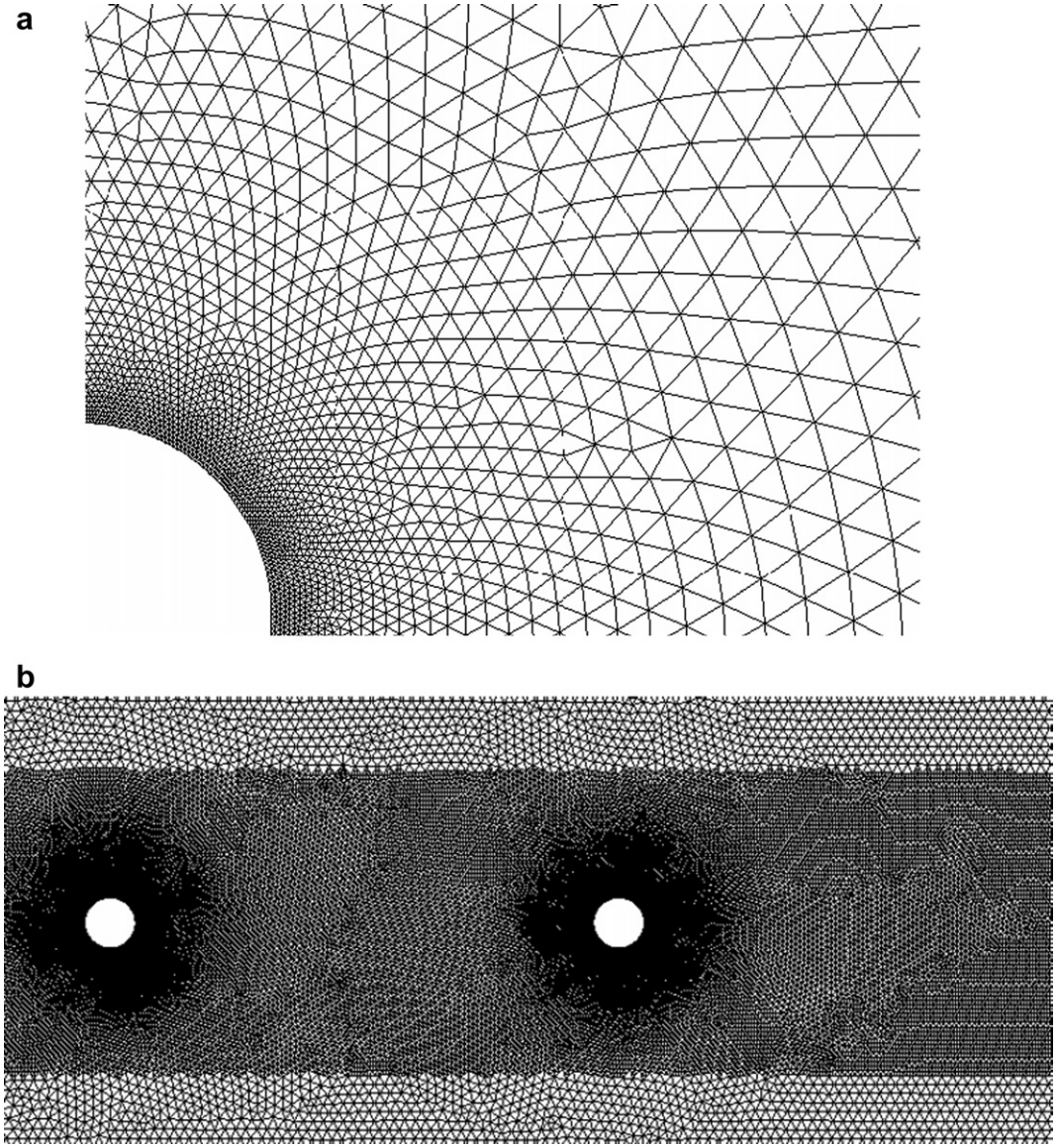

Fig. 2. Typical grid structure used in the study: (a) around a cylinder, (b) along the flow direction.

Table 1
The convergence of the second order time stepping scheme for key parameters at $Re = 200$

Δt	St	C_D	C_L	Nu
0.01	0.192	1.368 ± 0.051	±0.702	7.469 ± 0.030
0.05	0.192	1.376 ± 0.048	±0.698	7.474 ± 0.028
0.10	0.205	1.382 ± 0.047	±0.719	7.481 ± 0.027

Table 2
Comparison of the average drag coefficient and Strouhal number for a single cylinder at $Re = 100$

	St	C_D	C_L
Present study	0.172	1.368 ± 0.029	±0.343
Meneghini et al. (2001)	0.165	1.37	
Braza et al. (1986)	0.160	1.364 ± 0.015	±0.25
Ding et al. (2007)	0.166	1.356 ± 0.010	±0.287
Meneghini (1993)	0.162	1.52	
Sa and Chang (1991)	0.155	1.23	
Liu et al. (1998)	0.164	1.35 ± 0.012	±0.339
Saltara (1999)	0.160	1.33	
Experimental			
Williamson (1991)	0.164		
Roshko (1954)	0.16–0.17		
Norberg (2003)	0.168		±0.18 to ±0.54
Tritton (1959)		1.25	

From the heat transfer point of view, the mean Nusselt number of a single isothermal cylinder in cross flow of air was computed and compared with the values obtained from the following correlations available in the literature:

Zhuauskas (1972) correlation

$$Nu = 0.51\,Re^{0.5} \tag{8}$$

Knudsen and Katz (1958)

$$Nu = 0.683 Re^{0.466}\, Pr^{1/3} \tag{9}$$

Churchill and Bernstein (1977) correlation

Table 3
Comparison of the average drag coefficient and Strouhal number for a single cylinder at $Re = 100$

	St	C_D	C_L
Present study	0.192	1.376 ± 0.048	±0.698
Meneghini (1993)	0.196	1.25	
Borthwick (1986)	0.188	1.02	
Braza et al. (1986)	0.200	1.40 ± 0.05	±0.75
Arkell (1995)	0.196	1.30	
Liu et al. (1998)	0.192	1.31 ± 0.049	±0.69
Belov et al. (1995)	0.193	1.19 ± 0.042	±0.64
Ding et al. (2007)	0.196	1.348 ± 0.050	±0.659
Saltara (1999)	0.190	1.25	
Experimental			
Williamson (1991)	0.196		
Roshko (1954)	0.17–0.19		
Norberg (2003)	0.18–0.197		±0.35 to ±0.70

$$Nu = 0.3 + \frac{0.62 Re^{1/2} Pr^{1/3}}{[1 + (0.4/Pr)^{2/3}]^{1/4}} \left[1 + \left(\frac{Re}{282000}\right)^{5/8}\right]^{4/5} \tag{10}$$

In Table 4, the mean Nusselt number computed using FLUENT and the numerical values obtained from aforementioned correlations were comparatively tabulated for $Re = 100$, 150 and 200. The mean Nusselt number for $Re = 100$ agrees very well with the predictions of all three correlations. As the Reynolds number is increased beyond 100, the FLUENT solutions for the mean Nusselt number result in about 2% and 4% higher in values for $Re = 150$ and 200, respectively.

Table 4
Comparison of the mean Nusselt numbers for a single cylinder as a function of Reynolds number

The mean Nusselt number				
Re	Present	Eq. (8)	Eq. (9)	Eq. (10)
100	5.179 ± 0.003	5.10	5.19	5.16
150	6.383 ± 0.022	6.25	6.26	6.26
200	7.474 ± 0.028	7.21	7.16	7.19

Table 5
Flow parameters from the present study at $Re = 100$ and 200 and comparisons with available literature data

Re	*L/D*	$C_{D,1}$	$C_{L,1}$	St_1	$C_{D,2}$	$C_{L,2}$
100	2	1.225	±0.0075		±0.00012	±0.0258
	2.5	1.386 ± 0.011[a]	±0.37	0.169	−0.075	0
	3	1.205	0		−0.048	0.0014 ± 0.004
	4	1.345 ± 0.0243	±0.478	0.156	0.764 ± 0.204	±1.455
	5	1.369 ± 0.013	±0.437	0.161	0.874 ± 0.165	±1.617
	5.5	1.433 ± 0.015[a]	±0.403	0.168	0.952 ± 0.164	±1.741
	7	1.355 ± 0.014	±0.363	0.166	0.682 ± 0.07	±1.309
	10	1.383 ± 0.011	±0.359	0.172	0.731 ± 0.087	±1.14
200	2	1.06 ± 0.0004	±0.034		−0.21 ± 0.0036	±0.17
		0.89 ± 0.05[b]	±0.20	0.130	−0.21 ± 0.15	
		1.03[c]		0.130	−0.17	
	3	1.051 ± 0.025	±0.029	0.130	−0.56 ± 0.012	±0.269
		0.87 ± 0.05[b]	±0.10		−0.16 ± 0.15	±0.30
		1.0[c]		0.125	−0.08	
	4	1.34 ± 0.056	±0.805	0.181	0.558 ± 0.22	±1.99
		1.11 ± 0.05[b]	±0.70	0.190	0.88 ± 0.40	±1.80
		1.18[c]		0.174	0.38	
	5	1.327 ± 0.055	±0.731	0.186	0.455 ± 0.16	±1.569
		0.97 ± 0.05[b]	±0.55	0.180	0.70 ± 0.30	±1.60
	7	1.356 ± 0.049	±0.742	0.194	0.442 ± 0.15	±1.328
		1.09 ± 0.05[b]	±0.60	0.190	0.60 ± 0.35	±1.60
	10	1.359 ± 0.054	±0.70	0.191	0.524 ± 0.153	±1.287
		1.30 ± 0.05[b]	±0.70	0.200	0.90 ± 0.40	±1.90

[a] Mittal et al. (1997).
[b] Slaouti and Stansby (1992).
[c] Meneghini et al. (2001).

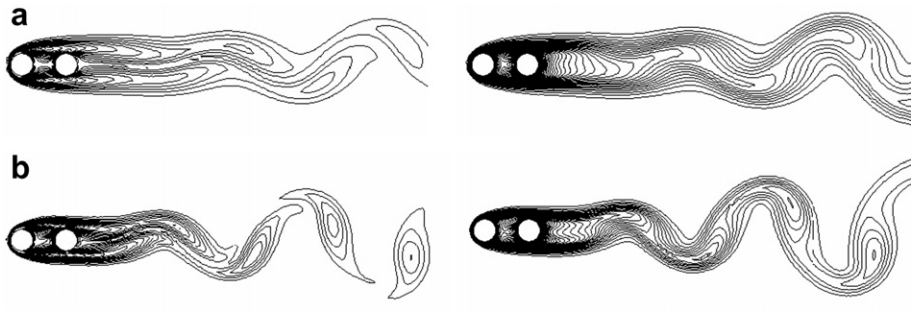

Fig. 3. Vorticity (on the left) and isotherms (on the right) for tandem arrangement of two cylinders with $L/D = 2$: (a) $Re = 100$, (b) $Re = 200$.

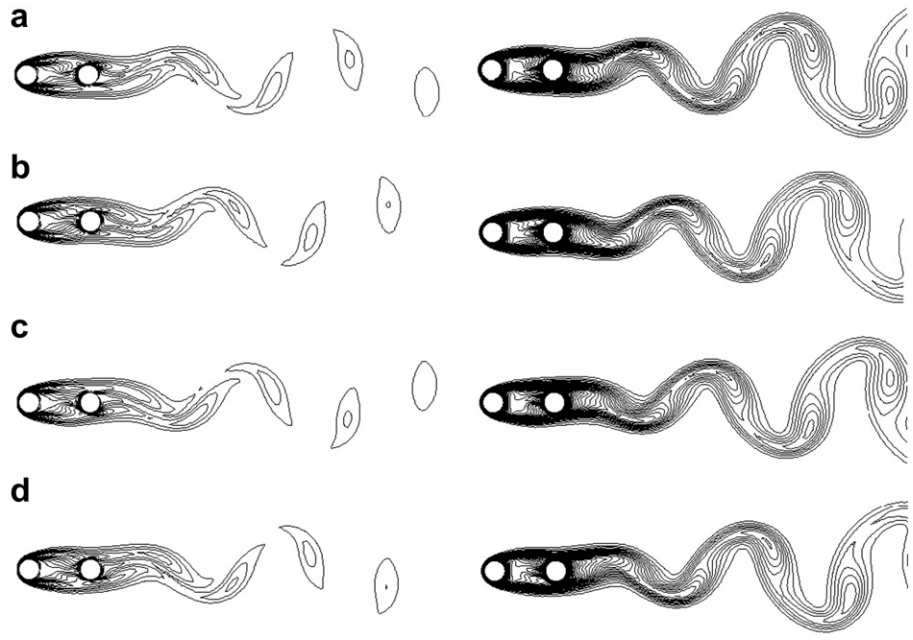

Fig. 4. Vorticity (left) and isotherms (right) for tandem arrangement of two cylinders during one period of vortex formation for $L/D = 3$ and $Re = 200$: (a) $T/4$, (b) $2T/4$, (c) $3T/4$, (d) T.

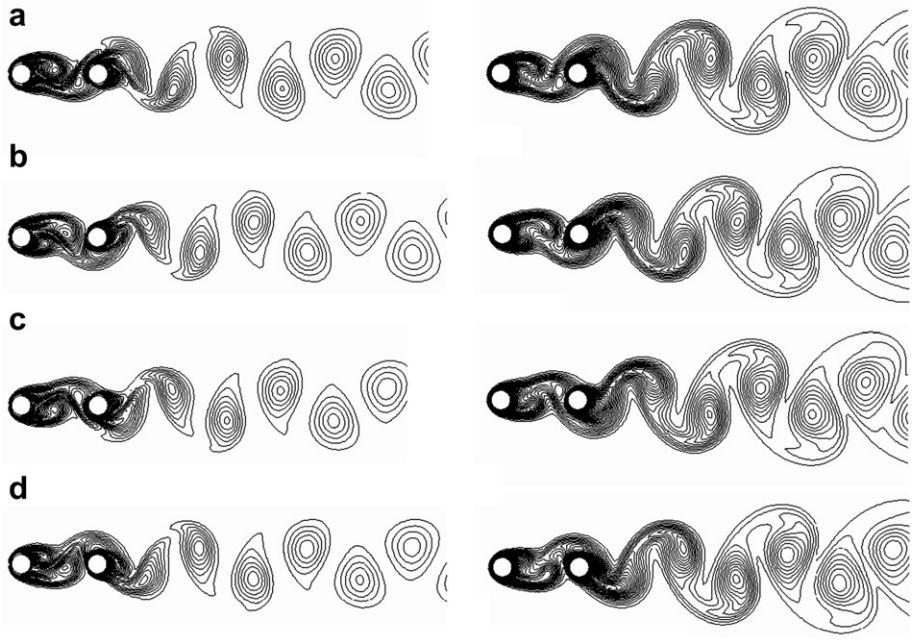

Fig. 5. Vorticity (left) and isotherms (right) for tandem arrangement of two cylinders during a complete vortex shedding cycle for $L/D = 4$ and $Re = 100$: (a) $T/4$, (b) $2T/4$, (c) $3T/4$, (d) T.

A second case for FLUENT verification is the air flow over two cylinders in tandem arrangement. A rectangular computational domain of height $20D$ and length $28.5D + L$ is considered (Fig. 1). In this study, the number of nodes varied from approximately 28150 for $L/D = 2$ to 36890 for $L/D = 10$. The Strouhal number, lift and drag coefficients for $L = 2D$, $3D$, $4D$, $5D$, $7D$ and $10D$ were obtained and compared with the available data in the literature.

In Table 5, the flow parameters for $Re = 100$ and 200 and for various tandem arrangements are provided. For $Re = 100$, flow parameters for $L/D = 2.5$ and 5.5 (Mittal et al., 1997) was also tabulated since these were the only data found in the literature. The Strouhal numbers for both cylinders are the same; thus, the Strouhal number for upstream cylinder only is provided in Table 5. The numerical solutions of Mittal et al. (1997) are higher than those of the present study. For $Re = 200$, the flow parameters obtained from the present study are compared with those of Meneghini et al. (2001) and Slaouti and Stansby (1992). Considering the oscillation amplitudes of the lift and drag coefficients, the agreement between the flow parameters, especially the Strouhal numbers, are very good.

4. Results and discussion

4.1. Isotherms and vorticity contours

Zdravkovich (1977) reported that three major flow regimes can be observed for the cylinders placed in tandem: (a) the extended-body regime ($L/D < 1.2 - 1.8$), (b) the reattachment regime, ($1.2 - 1.8 < L/D < 3.4 - 3.8$) and (c) the co-shedding regime ($L/D > 4$). A wide range of studies reveal that the critical spacing for vortex formation between the cylinders is about $\sim 3.5D - 3.8D$.

In Fig. 3, the vortex structure and the isotherms are depicted for $Re = 100$, $Re = 200$ and $L/D = 2$. For $Re = 100$, Fig. 3a, a vortex formation between the two cylinders is not observed; however, the flow oscillates further downstream of the second cylinder. For $Re = 200$, Fig. 3b, the oscillations increase to form a vortex street at the downstream region. As both the vorticity and the thermal energy are transported by the flow, the vorticity contours and the isotherms exhibit similar features.

In Fig. 4, vortex formation and isotherms occurring for a complete vortex shedding cycle for $L/D = 3$ is illustrated. The center-

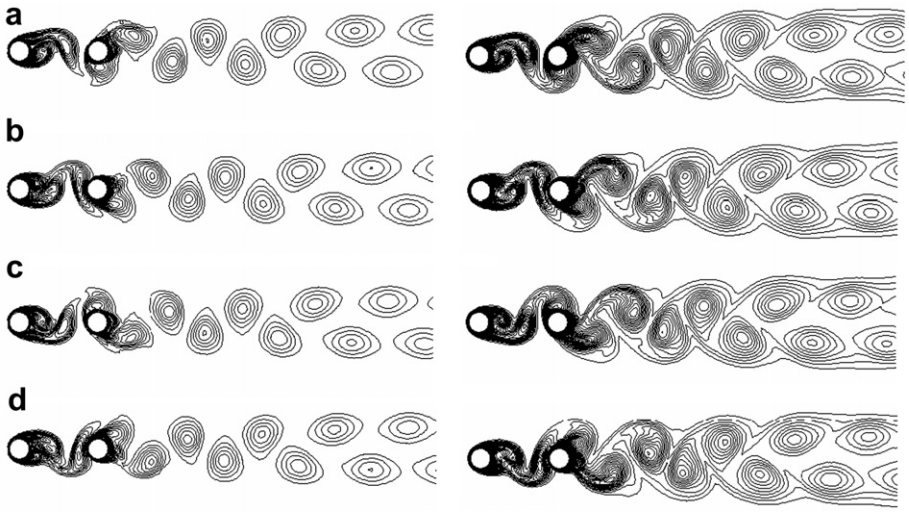

Fig. 6. Vorticity (on the left) and isotherms (on the right) for tandem arrangement of two cylinders during a complete vortex shedding cycle for $L/D = 4$ and $Re = 200$: (a) $T/4$, (b) $2T/4$, (c) $3T/4$, (d) T.

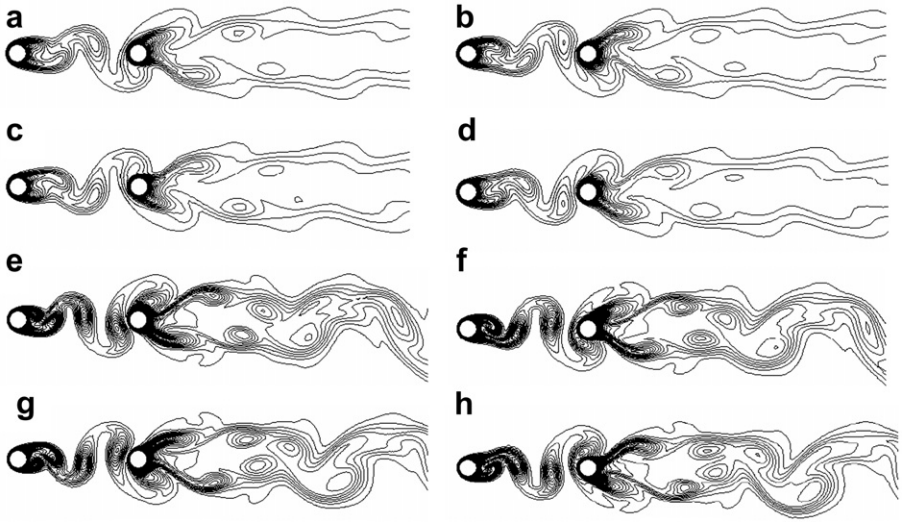

Fig. 7. Isotherms for$L/D = 7$ tandem arrangement of two cylinders during a complete vortex shedding cycle for $Re = 100$: (a) $T/4$, (b) $2T/4$, (c) $3T/4$, (d) T; and $Re = 200$: (e) $T/4$, (f) $2T/4$, (g) $3T/4$, (h) T.

to-center spacing is still below the critical value. Separated shear layer from upstream cylinder forms a vortex behind downstream cylinder. Energy is similarly transported by the fluid flow to the downstream region.

For the center-to-center spacing larger than the critical value, separated shear layers from both upstream cylinder and downstream cylinders form a vortex street. Figs. 5 and 6 depict the vortex structures and the isotherms between two cylinders and

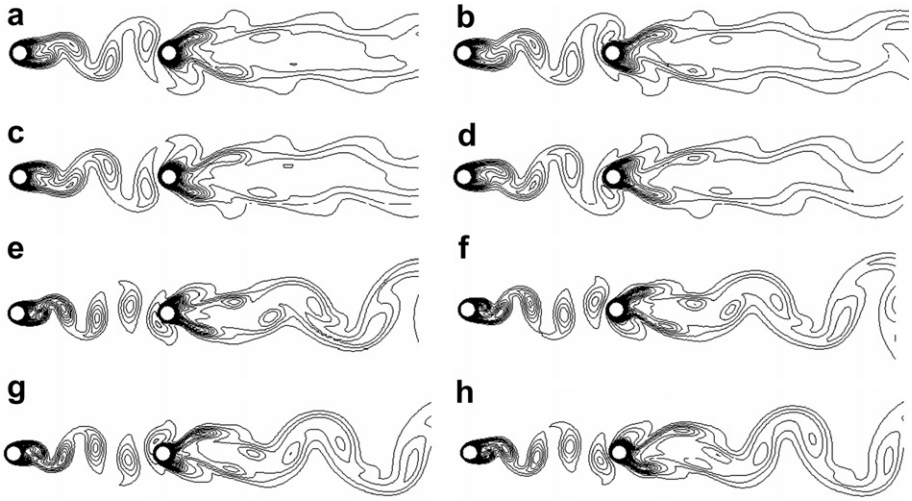

Fig. 8. Isotherms for $L/D = 10$ tandem arrangement of two cylinders during a complete vortex shedding cycle for $Re = 100$, (a) $T/4$, (b) $2T/4$, (c) $3T/4$, (d) T, and $Re = 200$, (e) $T/4$, (f) $2T/4$, (g) $3T/4$, (h) T.

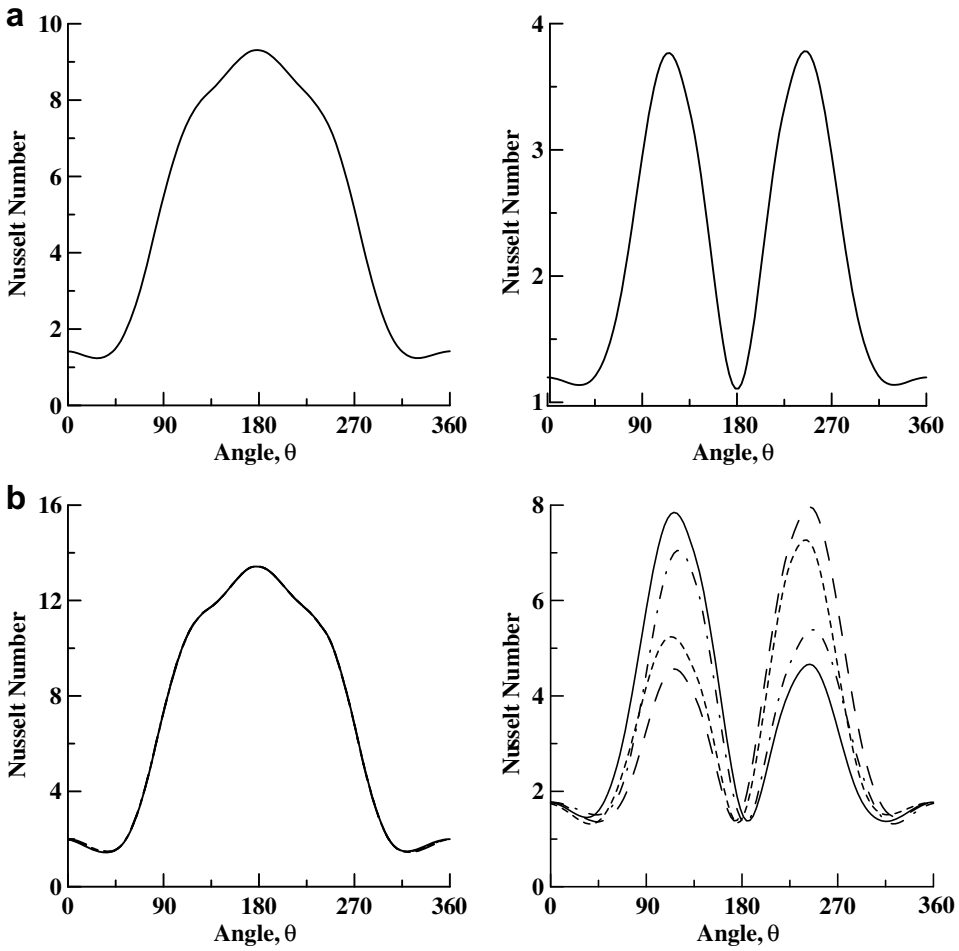

Fig. 9. The local Nusselt number distributions on the upstream (on the left) and downstream (on the right) cylinders in tandem arrangement for $L/D = 3$: (a) $Re = 100$, (b) $Re = 200$ during a complete vortex shedding cycle (— $T/4$, --- $2T/4$, – – $3T/4$, –·– T).

downstream region during a complete vortex shedding cycles for $L/D = 4$, $Re = 100$ and 200, respectively. Separated shear layer from downstream cylinder and impinging of vortex formed from upstream cylinder drastically increases heat transfer on downstream one. Both the flow field and the isotherms present similar features.

In Figs. 7 and 8, the isotherms for a complete shedding cycle for $Re = 100$ and 200 and for $L/D = 7$ and 10 are presented. These represent typical cases of co-shedding regime. The vortex street is established; however, the interactions within the vortex street with the shear layer separated from downstream cylinder create two separate vortices near the downstream cylinder. Further downstream, these vortices amalgamate and form the vortex street. For $Re = 200$, the magnitude of the vortices increase due to faster moving fluid, and shedding gains strength.

4.2. Local Nusselt number variations

One of the main objectives in heat transfer calculations is to determine the local and total heat transfer from isothermal cylinders. The effect of the flow structure especially on heat transfer can best be observed by analyzing the local heat transfer coefficient (or the local Nusselt number). The distribution of the local Nusselt number on a circular cylinder in a free stream was illustrated by Karanth et al. (1994). It is observed that the maximum rate of heat transfer occurs at the upstream stagnation point while the minimum heat transfer is observed between the boundary separation points and the downstream stagnation point ($\theta \approx 53^\circ$ and 308°). In Fig. 9, for $L/D = 3$, $Re = 100$ and 200, the local Nusselt number distributions along the perimeter of both the upstream and the downstream cylinders are provided. For $L/D = 3$, although the local Nusselt number profile of the upstream cylinder is similar to that of an isolated cylinder, the downstream cylinder exhibits a completely different characteristics. Since heat transfer rate is closely related to flow structure, the minima of the local heat transfer rates appear in the front and back stagnation points of the downstream cylinder where the velocity magnitudes are relatively small. Thus, in Fig. 9a, the maximum heat transfer from the downstream cylinder exhibits itself with a double hump occurring at $\theta \approx 115^\circ$ and 265° of the cylinder wall where the thermal and hydrodynamic boundary layers become the thinnest. The vortex formation at the downstream region coincides with the oscillation of the mean Nusselt number from large amplitude to the low amplitude during one period of vortex shedding for $L/D = 3$ and $Re = 200$ as seen in Fig. 9b.

In Fig. 10, the local Nusselt number along the cylinder perimeters during a complete vortex shedding cycle are depicted for $L/D = 4$, $Re = 100$ and 200. For $Re = 100$, the local Nusselt profiles of the upstream cylinder are completely symmetrical, but the profiles especially behind the upstream cylinder slightly change during one cycle. This phenomena is more visible, especially, at $Re = 200$ case,

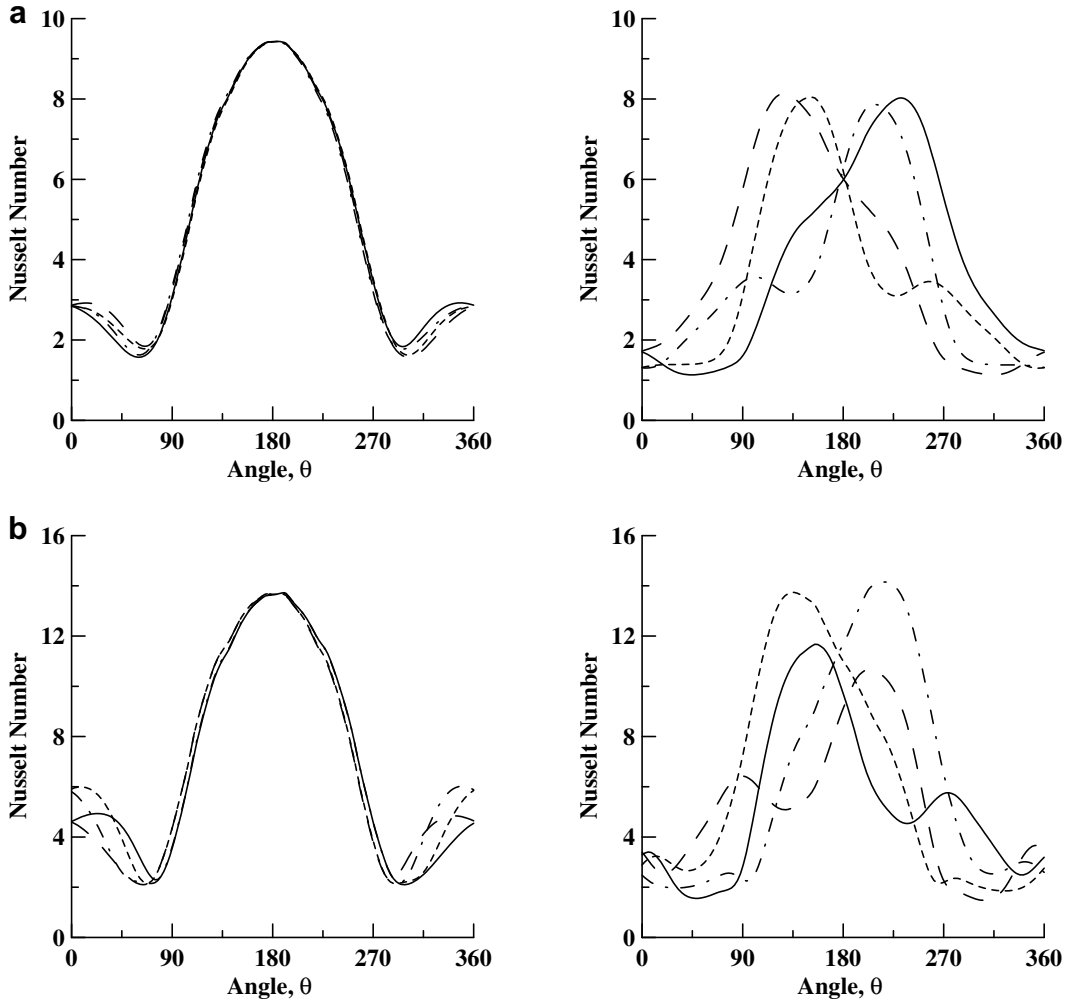

Fig. 10. The local Nusselt number distributions on the upstream (on the left) and downstream (on the right) cylinders in tandem arrangement for $L/D = 4$: (a) $Re = 100$, (b) $Re = 200$ during a complete vortex shedding cycle (— $T/4$, --- $2T/4$, – – $3T/4$, –·– T).

in Fig. 10b, due to an increase in the magnitude of the vortex shedding; however, the local Nusselt distribution still remains symmetrical. On the other hand, in the downstream cylinder, more dramatic changes are observed due to impinging vortex onto it. As it can be seen from Fig. 4 ($T/4$, $2T/4$, $3T/4$ and T), the vortex in between the two cylinders shifts periodically, causing the locations of not only the separation but also the stagnation points to be periodically displaced as well. Although, at $Re = 100$, the magnitude of the maximum heat transfer rate remains the same, its location follows the separation point where the boundary layer is the thinnest (Fig. 5). However, for $Re = 200$ in Fig. 10b, the local Nusselt number profile featuring a double hump structure and its magnitude within a shedding period varies in connection with the flow pattern (Fig. 6).

In Fig. 11, the local Nusselt number along both cylinder walls are illustrated for $L/D = 10$, $Re = 100$ and 200. The upstream cylinder exhibits a typical local Nusselt number distribution of a single cylinder for both $Re = 100$ and 200 with slight deviations at the stagnation point behind the cylinder. Even though the local Nusselt number distribution of the downstream cylinder resembles to that of upstream cylinder typified with a large hump, its magnitude is smaller than that of the upstream cylinder indicating less heat transfer from the downstream cylinder. The location of the maximum heat transfer at $Re = 200$ shifts from $\theta \approx 130^\circ$ to 220° during a complete vortex cycle.

4.3. Mean nusselt numbers

For $L/D \geqslant 4$, the mean Nusselt number oscillates periodically in time due to vortex shedding from one or both cylinders depending upon the Reynolds number. However, the amplitude of the oscillation depends on the Reynolds number and L/D ratio. For instance, for low Reynolds numbers, the amplitude is either relatively very small or nonexistent. In Table 6, for $Re = 100$ and 200, the mean Nusselt numbers for the upstream (Nu_1) and downstream (Nu_2) cylinders with their oscillating amplitudes are tabulated as a function of L/D ratio. For $Re = 100$, the mean Nusselt number for both the upstream and downstream cylinders, which do not oscillate, increases up to $L/D = 4$. For $L/D \geqslant 4$, the mean Nusselt values for both cylinders are almost constant; that is, $Nu_1 \cong 5.17$ and $Nu_2 \cong 4.27$. On the other hand, for $Re = 200$, the mean Nusselt numbers for the upstream and downstream cylinders similarly increase up to $L/D = 4$. A meaningful oscillation is observed in the downstream cylinder for $L/D = 4$. For $L/D \geqslant 4$, the mean Nusselt values for both cylinders are nearly constant; that is, $Nu_1 \cong 7.44$ and $Nu_2 \cong 5.9$. It can be noted that the mean Nusselt values for the upstream cylinder approaches to that of a single cylinder (see Table 4) for $L/D \geqslant 4$. However, although the mean Nusselt values of the downstream cylinder for $L/D \geqslant 4$ level out at about 5.9 value, this value is smaller than that of the upstream cylinder. Numerically speaking, the convective heat losses from the downstream cylinder

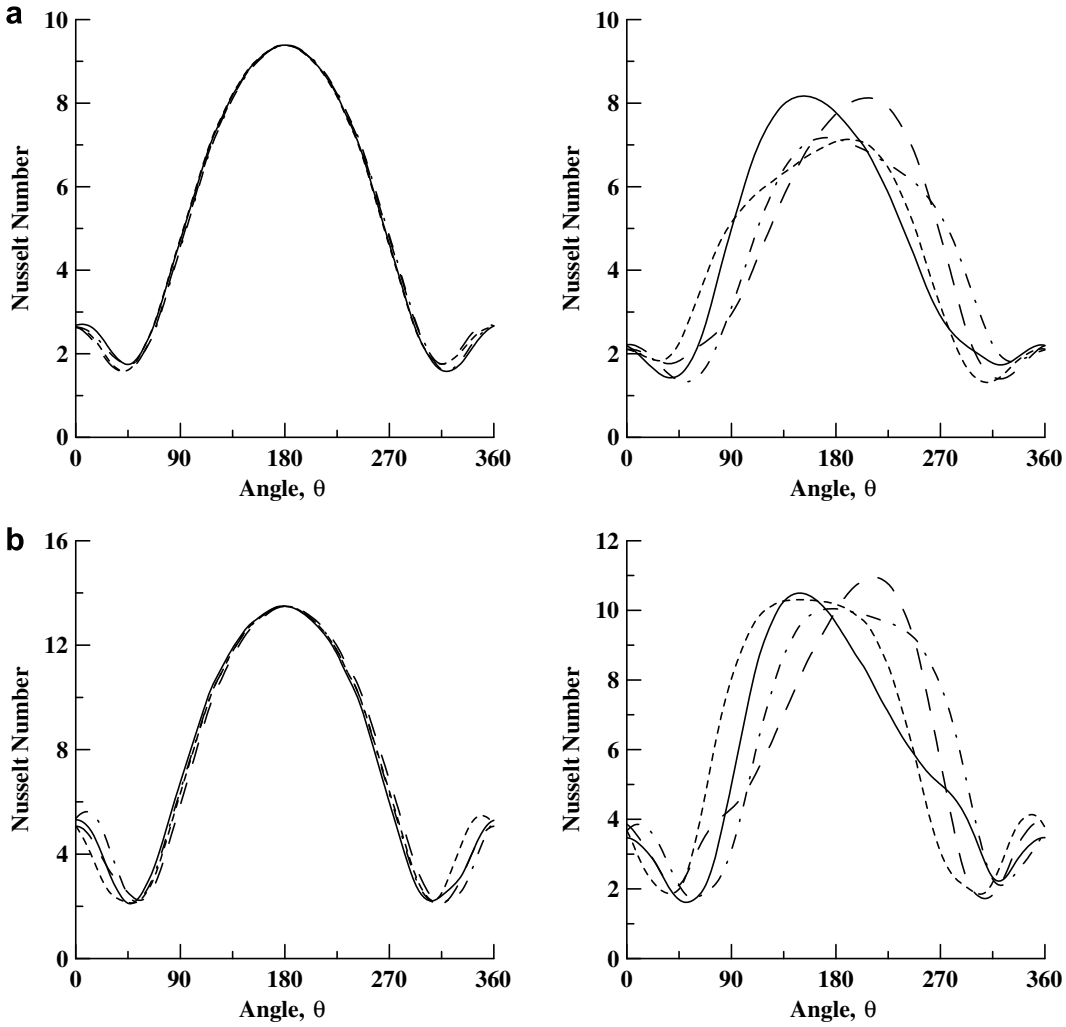

Fig. 11. The local Nusselt number distributions on the upstream (on the left) and downstream (on the right) cylinders in tandem arrangement for $L/D = 10$: (a) $Re = 100$, (b) $Re = 200$ during a complete vortex shedding cycle (— $T/4$, --- $2T/4$, – – $3T/4$, –·– T).

Table 6
The mean Nusselt numbers for the upstream and downstream cylinders as a function of Reynolds number and L/D ratio

Re	L/D	Nu_1	Nu_2
100	2	4.74	2.03
	3	4.804	2.293
	4	5.176 ± 0.006	4.02 ± 0.43
	5	5.180 ± 0.005	4.28 ± 0.40
	7	5.159 ± 0.003	4.21 ± 0.26
	10	5.174 ± 0.003	4.27 ± 0.18
200	2	6.460	2.88 ± 0.03
	3	6.56 ± 0.001	3.54 ± 0.11
	4	7.44 ± 0.046	6.15 ± 0.51
	5	7.43 ± 0.034	5.96 ± 0.47
	7	7.45 ± 0.029	5.83 ± 0.32
	10	7.46 ± 0.027	5.86 ± 0.26

decrease by about 20% due to the flow structure caused by the upstream cylinder.

5. Conclusions

Laminar unsteady convective heat transfer from two tandem cylinders subjected to cross flow of air is numerically investigated using FLUENT®. The flow and energy equations are solved for the Re = 100 and 200 and for L/D = 2, 3, 4, 5, 7 and 10. The flow parameters such as the Strouhal numbers, lift and drag coefficients are obtained and compared with the available literature to verify the code findings. The vorticity and isotherms were obtained to understand and interpret the flow and heat transport. In addition to the mean Nusselt numbers, the local Nusselt numbers along the perimeter of the upstream and downstream cylinders were obtained. It was observed that for high Reynolds flows the local Nusselt numbers of the downstream cylinder exhibits a double hump. The mean Nusselt number of the upstream cylinder approaches to that of a single cylinder for $L/D \geqslant 4$. As the heat transfer rate of the upstream cylinder approaches to that of a single cylinder, the heat transfer rate from the downstream cylinder is about 80% of that of the upstream cylinder.

References

Arkell, R., 1995. Wake dynamics of cylinders encountering free surface gravity waves. PhD Thesis, University of London, UK.

Belov, A., Martinelli, L., Jameson, A., 1995. A new implicit algorithm with multigrid for unsteady incompressible flow calculation. AIAA 95-0049 January.

Blevins, R., 1990. Flow-Induced Vibration. Van Nostrand Reinhold, New York.

Borthwick, A., 1986. Comparison between two finite-difference schemes for computing the flow around a cylinder. Int. J. Numer. Meth. Fluids 6, 275–290.

Braza, M., Chassaing, P., Ha Minh, H., 1986. Numerical study and physical analysis of the pressure and velocity fields in the near wake of a circular cylinder. J. Fluid Mech. 165, 79–130.

Buyruk, E., 2002. Numerical study of heat transfer characteristics on tandem cylinders, inline and staggered tube bank in cross-flow of air. Int. Commun. Heat Mass Transfer 29 (3), 355–366.

Carmo, B.S., Meneghini, J.R., 2006. Numerical investigation of the flow around two circular cylinders in tandem. J. Fluids Struct. 22, 979–988.

Chen, S.S., 1987. Flow-Induced Vibration of Circular Cylindrical Structures. Hemisphere Publishing Company, Washington.

Churchill, S.W., Bernstein, M.J., 1977. A correlating equation for forced convection from gases and liquids to a circular cylinder in crossflow. J. Heat Transfer 99, 300–306.

Ding, H., Shu, C., Yeo, Y.O., Xu, D., 2007. Numerical simulation of flows around two circular cylinders by mesh-free least square-based finite difference methods, Int. J. Numer. Meth. Fluids 53, 305–332.

Farrant, T., Tan, M., Price, W.G., 2001. A cell boundary element method applied to laminar vortex shedding from circular cylinders. Comput. Fluids 30, 211–236.

Fletcher, C.A.J., 1991. Computational Techniques for Fluid Dynamics. Springer-Verlag Berling Heidelberg, Germany.

FLUENT, Inc., FLUENT 6.1 User's Guide, 2003, Lebanon: NH.

Jue, T.C., Wu, H.W., Huang, S.Y., 2001. Heat transfer predictions around three heated cylinders between two parallel plates. Numer. Heat Transfer A 40, 715–733.

Karanth, D., Rankin, G.W., Sridhar, D., 1994. A finite difference calculation of forced convective heat transfer from an oscillating cylinder. Int. J. Heat Mass Transfer 37 (11), 1619–1630.

King, R., Johns, D., 1976. Wake interaction experiments with two flexible circular cylinders in flowing water. J. Sound Vib. 45, 259–283.

Knudsen, J.D., Katz, D.L., 1958. Fluid Dynamics and Heat Transfer. McGraw Hill, New York.

Kostic, Z.G., Oka, S.N., 1972. Fluid flow and heat transfer with two cylinders in cross flow. Int. J. Heat Mass Transfer 15, 279–299.

Kondo, N., Matsukuma, D., 2005. Numerical simulation for flow around two circular cylinders in tandem. Int. J. Comput. Fluid Dyn. 19 (4), 277–288.

Liu, C., Zheng, X., Sung, C.H., 1998. Preconditioned multigrid methods for unsteady incompressible flows. J. Comput. Phys. 139, 35–37.

Meneghini, J.R., 1993. Numerical simulation of bluff body flow control using a discrete vortex method. PhD thesis, University of London, UK.

Meneghini, J.R., Saltara, F., Siqueira, C.L.R., Ferrari, J.A., 2001. Numerical simulation of flow interference between two circular cylinders in tandem and side-by-side arrangements. J. Fluids Struct. 15, 327–350.

Mittal, S., Kumar, V., Raghuvanshi, A., 1997. Unsteady incompressible flows past two cylinders in tandem and staggered arrangements. Int. J. Numer. Meth. Fluids 25, 1315–1344.

Norberg, C., 2003. Fluctuating lift on a circular cylinder: review and new measurements. J. Fluids Struct. 17, 57–96.

Patankar, S.V., 1980. Numerical Heat Transfer and Fluid Flow. Hemisphere, Washington, DC.

Rahnama, M., Hadi-Moghaddam, H., 2005. Numerical investigation of convective heat transfer in unsteady laminar flow over a square cylinder in a channel. Heat Transfer Eng. 26 (10), 21–29.

Roshko, A., 1954. On the drag and shedding frequency of two dimensional bluff bodies. Technical Note 3169, National Advisory Committee for Aeronautics (NACA), Washington.

Sa, J.Y., Chang, K.S., 1991. Shedding patterns of the near-wake vortices behind a circular cylinder. Int. J. Numer. Meth. Fluids 12, 463–474.

Saltara, F., 1999. Numerical Simulation of the flow about circular cylinders. PhD thesis, EPUSP University of Sao Paulo, Brazil (in Portuguese).

Slaouti, A., Stansby, P.K., 1992. Flow around two circular cylinders by the random-vortex method. J. Fluids Struct. 6, 641–670.

Sumner, D., Price, S.J., Paidoussis, M.P., 2000. Flow-pattern identification for two staggered circular cylinders in cross-flow. J. Fluid Mech. 411, 263–303.

Tanida, Y., Okajima, A., Watanabe, Y., 1973. Stability of a circular cylinder oscillating in uniform flow or in a wake. J. Fluid Mech. 41, 769–784.

Tritton, D.J., 1959. Experiments on the flow past a circular cylinder at low Reynolds numbers. J. Fluid Mech. 6, 547–567.

Williamson, C.H.K., 1991. 2-D and 3-D aspects of the wake of a cylinder and their relation to wake computations. In: Anderson, C.R., Greengard, C. (Eds.), Vortex Dynamics and Vortex Methods, vol. 28. American Mathematical Society, pp. 719–751. Lectures in Applied Mathematics.

Zdravkovich, M.M., 1977. Review of flow interference between two circular cylinders in various arrangements. Trans. ASME J. Fluids Eng. 99, 618–633.

Zdravkovich, M.M., 1985. Flow induced oscillations of two interfering circular cylinders. J. Sound Vib. 101 (4), 511–521.

Zhou, Y., Yiu, M.W., 2006. Flow structure, momentum and heat transport in a two-tandem-cylinder wake. J. Fluid Mech. 548, 17–48.

Zhuauskas, A., 1972. Heat transfer from tubes in cross-flow. In: Harnett, J.P., Irwine, T.F. (Eds.), Advances in Heat Transfer, vol. 8. Academic Press, New York.